Rapid Measurement of Protein Osmotic Second Virial Coefficients by Self-Interaction Chromatography

Peter M. Tessier, Abraham M. Lenhoff, and Stanley I. Sandler
Center for Molecular and Engineering Thermodynamics, Department of Chemical Engineering, University of Delaware, Newark, Delaware 19716

ABSTRACT Weak protein interactions are often characterized in terms of the osmotic second virial coefficient (B_{22}), which has been shown to correlate with protein phase behavior, such as crystallization. Traditional methods for measuring B_{22}, such as static light scattering, are too expensive in terms of both time and protein to allow extensive exploration of the effects of solution conditions on B_{22}. In this work we have measured protein interactions using self-interaction chromatography, in which protein is immobilized on chromatographic particles and the retention of the same protein is measured in isocratic elution. The relative retention of the protein reflects the average protein interactions, which we have related to the second virial coefficient via statistical mechanics. We obtain quantitative agreement between virial coefficients measured by self-interaction chromatography and traditional characterization methods for both lysozyme and chymotrypsinogen over a wide range of pH and ionic strengths, yet self-interaction chromatography requires at least an order of magnitude less time and protein than other methods. The method thus holds significant promise for the characterization of protein interactions requiring only commonly available laboratory equipment, little specialized expertise, and relatively small investments of both time and protein.

INTRODUCTION

Understanding weak protein interactions is important for treating biological disorders (Hirsch et al., 1988; Zhang and Augusteyn, 1994), crystallizing proteins (Durbin and Feher, 1996), including for structure-based drug design (Oakley and Wilce, 2000), purifying protein mixtures (Mukai et al., 1998), understanding protein diffusion in concentrated solutions (Kuehner et al., 1997), and stabilizing protein therapeutic formulations (Cleland et al., 1993). However, these interactions are typically too weak to characterize in terms of quantities such as association constants that are suitable for strong protein interactions measured using methods such as surface plasmon resonance (Fagerstam et al., 1992) or fluorescence polarization (Freyssinet et al., 1978). Instead, weak protein interactions are often characterized in terms of the osmotic second virial coefficient (B_{22}), especially because it can be measured using traditional colloidal characterization techniques, such as static light scattering (SLS) (George and Wilson, 1994; Bonneté et al., 1999; Guo et al., 1999; Hitscherich et al., 2000), small-angle x-ray (Porschel and Damaschun, 1977; Ducruix et al., 1996) or neutron (Receveur et al., 1998; Velev et al., 1998) scattering, membrane osmometry (Haynes et al., 1992; Schaink and Smit, 2000), and sedimentation equilibrium (Behlke and Ristau, 1999). However, all of these methods are generally labor intensive and expensive in terms of both time and protein.

The need for a faster, less expensive method of measuring osmotic second virial coefficients has been stimulated by the recent pioneering correlation between B_{22} and crystallization conditions: solution conditions under which proteins have a propensity to crystallize correspond to slightly negative virial coefficients, resulting from weak attractive protein interactions (George and Wilson, 1994). This observation is significant because protein crystallization is critical to structural biology and often is the bottleneck in structure-based drug design. However, the crystallization community has largely ignored this approach of measuring virial coefficients because it requires several orders of magnitude more protein than is commonly available. Instead, crystallographers continue to use empirical crystallization screens, which provide little information when they fail. It would be more informative if the screening method could provide some indication of how close the solution conditions were to ones conducive to growing crystals; this would be possible with a more efficient method for method for measuring B_{22}.

Self-interaction chromatography (SIC) (Patro and Przybycien, 1996) is an alternative method of characterizing protein interactions that could potentially meet the requirements of being inexpensive in terms of both time and protein relative to other characterization techniques. The approach involves covalently immobilizing protein on chromatographic particles, packing the particles into a column, and measuring the retention time of a pulse of protein injected into the column under isocratic conditions; the relative retention reflects the average protein interactions. Although this method has previously been used to describe the destabilizing effects of additives on protein interactions qualitatively (Patro and Przybycien, 1996), we show in this work that SIC can be used to determine protein interactions quantitatively in terms of the osmotic second virial coefficient. We first develop a model relating the relative reten-

Submitted June 5, 2001, and accepted for publication December 7, 2001.
Address reprint requests to Dr. Abraham M. Lenhoff, University of Delaware, Department of Chemical Engineering, Newark, DE 19716. Tel.: 302-831-8989; Fax: 302-831-4466; E-mail: lenhoff@che.udel.edu.

0006-3495/02/03/1620/12 $2.00

tion to the osmotic second virial coefficient and then present experimental results that show that we are able to achieve quantitative agreement with virial coefficients measured by traditional characterization techniques.

THEORY

The interaction between two protein molecules in solution can be expressed in terms of the osmotic second virial coefficient (B_{22}) (Zimm, 1946; McQuarrie, 1976):

$$B_{22} = -\frac{1}{2}\int_{\Omega_2}\int_{\Omega_1}\int_0^\infty (e^{-W/kT} - 1) r_{12}^2 dr_{12} d\Omega_1 d\Omega_2 \quad (1)$$

The potential of mean force (PMF), W, describes the anisotropic interaction energy between two protein molecules in solution and is a function of all orientations and separation distances (r_{12}). Ω_1 and Ω_2 are normalized angular vectors describing the angular position and orientation of both molecules. The factor of 1/2 corrects for double counting of an identical pair of molecules. The integral in Eq. 1 can be split into excluded volume and intermolecular interaction contributions:

$$B_{22} = \frac{1}{2}\int_{\Omega_2}\int_{\Omega_1}\left[\frac{1}{3}r_c^3 - \int_{r_c}^\infty (e^{-W/kT} - 1) r_{12}^2 dr_{12}\right] d\Omega_1 d\Omega_2, \quad (2)$$

where $r_c(\Omega_1, \Omega_2)$ is the separation distance upon contact. This relationship assumes that both molecules sample all orientations, which differs from the experimental system in this work, where one of the two protein molecules is immobilized and therefore cannot sample all orientations. Thus, our goal in this section is to relate measurable chromatographic parameters to the PMF and ultimately to B_{22}.

Protein interactions that dominate the value of B_{22} have been shown to be short range in nature (Rosenbaum and Zukoski, 1996; Neal et al., 1998), typically persisting over a distance less than the diameter of the protein molecule at moderate ionic strengths (>0.1 M). An additional relevant length scale is that of the typical pore size of a chromatographic particle, which for protein applications is generally much larger than the size of a protein molecule. Therefore, we model immobilized protein molecules as being fixed to an effectively flat surface. Further, we assume that a free protein molecule interacts with only one immobilized protein molecule at a time (i.e., two-body interactions), again due to the short-range nature of protein interactions. The validity of this assumption will depend on the particle surface coverage (and therefore the intermolecular spacing) of the immobilized protein. Finally, the free protein molecules are assumed to interact only with the immobilized protein and not appreciably with each other, which can be achieved experimentally by using relatively low protein concentrations for the mobile phase sample.

Chromatographic retention is usually characterized experimentally in terms of the retention factor

$$k' = \frac{V_r - V_o}{V_o}, \quad (3)$$

where V_r is the retention volume, which is the average volume required to elute a solute from the column, and V_o is the retention volume for the situation where the free molecules do not interact with the surface of the particles. To develop a model that relates the retention factor to the interactions between free and immobilized protein molecules, we consider the column structure more explicitly, decomposing the column into a bed of particles that have an extra-particle or interstitial volume (V_i) and an intra-particle or pore volume (V_p). The retention volume can be written as

$$V_r = V_i + KV_p, \quad (4)$$

where K is the distribution coefficient, defined as (Ståhlberg et al., 1991)

$$K = \frac{c_p}{c_i} = \frac{\int_{V_p} e^{-\Delta G/kT} dV_p}{V_p}, \quad (5)$$

where c_p is the concentration of protein in the pore space and c_i is the concentration of protein in the interstitial volume, and ΔG is the free energy change of bringing protein into an arbitrary element of pore volume, dV_p, from the interstitial volume. The distribution coefficient is a measure of protein interactions, because $K > 1$ corresponds to the protein being enriched in the pore space and thus retained longer than the dead time of the column due to attractive interactions. Equations 3, 4, and 5 can be combined to give:

$$k' = \frac{(K-1)V_p}{V_o} = \frac{\int_{V_p}(e^{-\Delta G/kT} - 1) dV_p}{V_o} \quad (6)$$

The free energy change for transferring a single free molecule from the interstitial volume into the pore volume so that it interacts with a single immobilized molecule is equivalent to the PMF, evaluated at a given separation distance (r_{12}) and given orientations of both the free (Ω_1) and immobilized (Ω_2) molecules:

$$\Delta G(r_{12}, \Omega_1, \Omega_2) = W(r_{12}, \Omega_1, \Omega_2) \quad (7)$$

The equality of Eq. 7 is based on the identification of the PMF as the free energy required to bring together two solute molecules from infinitely far apart to a defined separation distance and orientation (Hill, 1960). The distribution coefficient for one free protein molecule interacting with one immobilized molecule, j, in a fixed orientation Ω_j, averaged

over all separation distances and orientations of the free protein, can then be written as:

$$K_j(\Omega_j) - 1 = \frac{\int_{\Omega_1}\int_{r_c}^{\infty} (e^{-W(r_{1j},\Omega_1,\Omega_j)/kT} - 1) r_{1j}^2 dr_{1j} d\Omega_1}{V_p} \quad (8)$$

The lower limit of the separation integral is taken as the separation distance upon contact, rather than zero, because $K_j(\Omega_j) - 1$ characterizes the intermolecular interactions relative to the excluded volume. The upper limit of the separation distance integral is taken as infinity rather than the pore diameter because the interaction energy is negligible beyond a distance of a few protein diameters, which will make the integrand equal to zero.

The total distribution coefficient can be obtained by summing over all immobilized molecules in the pore space, but the orientation of the immobilized molecules must also be considered. Most immobilization chemistries, including the one used in this work, involve linking ligands on the particle surface with primary amine groups on the protein surface. Globular proteins generally have several lysine groups on the surface and therefore are likely to be immobilized in random orientations (Patro and Przybycien, 1996). We assume that on average free protein molecules will interact with immobilized protein molecules displaying many different orientations. Thus, accounting for all the immobilized molecules and the randomness of their orientations is equivalent to integrating over the orientations of the N immobilized protein molecules (Ω_2):

$$K - 1 = \sum_{j=1}^{N} (K_j(\Omega_j) - 1) = N\langle K_j(\Omega_2) - 1\rangle = \frac{N \int_{\Omega_2}\int_{\Omega_1}\int_{r_c}^{\infty} (e^{-W(r_{12},\Omega_1,\Omega_2)/kT} - 1) r_{12}^2 dr_{12} d\Omega_1 d\Omega_2}{V_p} \quad (9)$$

Combining Eqs. 3, 4, and 9, the retention factor can be written as

$$k' = \frac{\frac{1}{2}\rho_s A_s \int_{\Omega_2}\int_{\Omega_1}\int_{r_c}^{\infty} (e^{-W(r_{12},\Omega_1,\Omega_2)/kT} - 1) r_{12}^2 dr_{12} d\Omega_1 d\Omega_2}{V_o}, \quad (10)$$

where ρ_s is the number of immobilized molecules per unit area, A_s is the total available surface area, and their product is the total number of immobilized protein molecules. The factor of ½ here accounts for the accessibility of only one side of the immobilized molecules.

By comparing Eq. 10 with Eq. 2, the second virial coefficient can be written as

$$B_{22} = B_{HS} - \frac{k'}{\rho_s \phi}, \quad (11)$$

where the phase ratio is defined to be $\phi = A_s/V_o$, and B_{HS} is the excluded volume or hard sphere contribution. Equation 11 provides a connection between the second virial coefficient and the retention factor based only on the size of the protein molecule, the amount of protein immobilized per unit area, and the phase ratio. These quantities can all be measured or calculated directly without the incorporation of adjustable parameters, as is shown later in a sample calculation.

MATERIALS AND METHODS

Materials

Chicken egg white lysozyme (three times crystallized, L-6876) and bovine pancreatic α-chymotrypsinogen A (six times crystallized, C-4879) were obtained from Sigma (St. Louis, MO) and stored below 0°C. Citric acid (ACS grade, C-1909), dibasic sodium phosphate (ACS grade, S-9390), bis-tris (B-7535), bis-tris propane (B-6755), ethanolamine (E-9508), calcium chloride (C-3881), sodium cyanoborohydride (S-8628), *N*-benzoyl-L-tyrosine ethyl ester (B-6125), and trizma hydrochloride (T-3253) were also purchased from Sigma. Potassium phosphate (ACS grade, P288), hydrochloric acid (ACS grade, A114–212), and sodium chloride (ACS grade, 5271) were purchased from Fisher. Glacial acetic acid was obtained from Mallinckrodt (3121). Magnesium bromide hexahydrate (21, 684–4) was obtained from Aldrich (Milwaukee, WI). Micro-BCA assay reagents (23231BP, 23232BP, and 23234BP) were obtained from Pierce. Toyopearl AF-Formyl-650M chromatography particles (08004) were obtained from Tosoh Biosep (formerly TosoHaas). All protein solutions and buffers were prepared with deionized water that was further purified using a Millipore Milli-Q system (>18.2 MΩ cm). The pH was adjusted using hydrochloric acid or sodium hydroxide and measured using a Chemcadet 5984 digital pH meter. Electrolyte solutions without protein were filtered through 0.22-μm Gelman bottle top filters (4632) into 2-L Corning sterile roller bottles (431133) and stored at room temperature. All protein solutions were filtered through 0.22-μm Millipore Millex-GV syringe filters (SLGVR25LS) just before use. All experiments were carried out at room temperature (23 ± 2°C). Protein concentrations were determined using a Perkin-Elmer Lambda 4B spectrophotometer at 280 nm, using an extinction coefficient of 2.64 L/g cm for lysozyme (Sophianopoulos et al., 1962) and 2.0 L/g cm for chymotrypsinogen (Smith, 1970).

Protein immobilization

Lysozyme was dissolved in 0.1 M potassium phosphate, pH 7.5, at 6.5 mg/ml. Chymotrypsinogen was dissolved in 1.0 M potassium phosphate (due to a low coupling yield at 0.1 M potassium phosphate), pH 8.5, at 9.8 mg/ml. Approximately 3 ml of Toyopearl AF-Formyl-650 M particles were washed with 250 ml of deionized water on a glass frit with a 0.2-μm Gelman membrane filter (60301). The particles were removed from the membrane and added to 10 ml of lysozyme or chymotrypsinogen solution. Approximately 90 mg of sodium cyanoborohydride was then added to the solution, and the vial was placed on a rotary mixer overnight. The particles were then washed with 200 ml of 0.1 and 1.0 M potassium phosphate solutions for lysozyme and chymotrypsinogen, respectively. The washed particles were added to ~15 ml of 1 M ethanolamine at pH 8, which was used to cap the remaining reactive groups. Approximately 20 mg of sodium cyanoborohydride was then added, and the particles were returned to the rotary mixer for 4 h. Finally, the particles were washed in 200 ml of 1 M sodium chloride solution at pH 7 to remove any unbound protein. The initial protein solution and the wash solutions were analyzed by UV spectrophotometry to determine the amount of bound protein. The amount of protein immobilized was also assayed directly by the micro-BCA method (Plant et al., 1991) and found to be within 20% of the total mass balance for the particles used to measure virial coefficient values. The

average immobilized concentrations of lysozyme and chymotrypsinogen were 14.4 and 21.3 mg protein/ml settled particles, respectively. Other lysozyme particles were also prepared to study the effects of surface coverage: 10 ml of 2.0 mg/ml lysozyme solution and 4 ml of particles yielded particles with 4 mg of lysozyme immobilized per ml of settled gel, 7 ml of 4.4 mg/ml lysozyme solution and 3 ml of particles yielded particles with 8 mg of lysozyme immobilized per ml of settled gel, and 10 ml of 10 mg/ml lysozyme solution and 2.5 ml of particles yielded particles with 17 mg lysozyme immobilized per ml of settled gel. The same reaction procedure was followed without protein to obtain particles that could be used to study protein-surface interactions. Also, it was found important not to use sodium azide as a preservative in the coupling buffer, even at very low concentrations (<0.02 wt %), because it significantly interfered with the coupling chemistry in cases where it was used. Finally, for proteins that are difficult to immobilize using this chemistry, see Battistel et al. (1991).

Self-interaction chromatography

Approximately 2.5 ml of a 50% slurry of particles with immobilized protein was packed into a 1-ml Waters AP glass mini-column (5 × 50 mm, 064–01) using an automated Pharmacia (Piscataway, NJ) FPLC system. The particles were packed at a maximum flow rate of 3 ml/min, and the flow rate was subsequently kept below 0.75 ml/min to insure that the bed would not settle further. The integrity of the column was confirmed by injecting 50 μl of a 1% solution of acetone, which typically gave a sharp, Gaussian peak. When the column was not being used, it was stored at 4°C in a low-salt buffer at pH 7 (lysozyme) or 3 (chymotrypsinogen), without a preservative (e.g., sodium azide).

Electrolyte solutions with and without 1 M sodium chloride were prepared in pairs for use in SIC. The electrolyte solutions were buffered at a concentration of 5 mM citric acid at pH 3, 5 mM acetic acid at pH 4.5, 5 mM sodium phosphate at pH 6, 5 mM bis-tris at pH 7, and 5 mM bis-tris propane at pH 9. The pH of these electrolyte solutions was stable to within ±0.05 pH units for ~24 h. For a given set of measurements, the pH would be held constant and, by blending the low- and high-salt solutions, the salt concentration could be varied. The electrolyte solutions were purged with helium for ~5 min before use. The outlet of the chromatography column was monitored by a UV detector at 280 nm. The column was equilibrated with both 0 and 1 M sodium chloride solutions for 10 column volumes or longer if necessary to reach a steady UV baseline at the beginning of each day.

Lysozyme and chymotrypsinogen solutions were prepared at concentrations of 20 and 1 mg/ml, respectively, using various concentrations of electrolyte. After the samples were pH adjusted and filtered, they were briefly sonicated (~10 s) to remove any air bubbles and then loaded into an auto-sampler. The FPLC system was computer controlled using FPLC Director software (version 1.1). The system was programmed to randomly inject 50-μl samples, each in triplicate, after 10 column volumes of equilibration at the desired salt concentration. After the protein was eluted, the salt concentration was increased to 1 M sodium chloride for ~4 column volumes, then decreased to 0 M sodium chloride for ~7 column volumes, and then finally adjusted to the next salt concentration of interest. The peak positions were analyzed digitally, and the retention volume was taken as the peak maximum.

Retention data processing

To calculate k', the dead volume (V_o), or the volume required for a noninteracting molecule the same size as a protein molecule to pass through the column, must be determined. It is not appropriate to measure the dead volume of the column using a small noninteracting molecule (e.g., acetone), because protein molecules access less of the pore space. To calculate the dead volume of the column with immobilized protein, we first measured the dead volume for a column of particles without protein immobilized using both acetone (V'_a) and protein (V'_p) (at 0.8 M NaCl to eliminate protein-surface interactions) in the mobile phase. An estimate of V_o for the column with protein immobilized can be found by multiplying the corresponding acetone dead volume by V'_p/V'_a. Finally, we subtracted the volume occupied by the immobilized protein molecules from the dead volume (which was not accounted for in the above procedure), which resulted in a small change in the virial coefficient values.

The protein diameter was calculated from the molecular volume of the protein (Neal and Lenhoff, 1995; Connolly, 1985, 1993), assuming the protein to be a sphere. We used a diameter of 3.11 nm for lysozyme and 3.84 nm for chymotrypsinogen. The excluded volume was calculated using the protein diameter ($B_{HS} = 2/3\pi d^3$ for spheres). The immobilized density (ρ_s) of protein was calculated by dividing the immobilized concentration (mass protein/particle volume) by the porosity (mobile phase volume/particle volume) and the phase ratio (surface area/mobile phase volume). Phase ratio data can be measured by inverse size exclusion chromatography and are available for dextran probes of various sizes for a variety of commercially available particles, including the particles used in this work (DePhillips and Lenhoff, 2000). The concentration of immobilized protein, which was taken as the average of the mass balance and the micro-BCA assay results, was calculated based on the settled particle volume. We corrected for the fact that the settled particle volume is ~20% greater than the packed particle volume by increasing the immobilized density accordingly. The phase ratio in Eq. 11 represents the available surface area/mobile phase volume, which is affected by the immobilized protein molecules. In view of the near-monolayer surface coverage attained for both proteins, we assumed that the amount of accessible surface area would be reduced proportionally by the size of the immobilized proteins. Assuming the pores to be cylindrical, we used a phase ratio in Eq. 11 based on the accessible pore space for pores of diameter greater than three protein diameters, which represents two molecules immobilized and one free molecule. A sample calculation is shown in Table 1.

TABLE 1 Key parameters for calculating a virial coefficient for lysozyme at pH 4.5 and 0.4 M NaCl

Description	Value
Retention factor, k'	0.076*
Mass protein/settled particle volume	14.4 mg/ml*
Mass protein/packed particle volume	17.3 mg/ml†
Column void volume/packed particle volume	0.811‡
Accessible surface area/mobile phase volume for $r = 1.55$ nm	20.9 m^2/ml§
Protein molecules/accessible surface area, ρ_s	4.3×10^{16} molecules/m^2
Accessible surface area/mobile phase volume for $r = 4.65$ nm, ϕ	16.9 m^2/ml§
Excluded volume, B_{HS}	6.24×10^{-20} cm^3 ‖
Second virial coefficient, B_{22}	-1.24×10^{-4} mol-ml/g^2

*Determined experimentally in this work.
†Immobilization density 20% greater for packed versus settled particle volume.
‡From DePhillips and Lenhoff (2000) for TosoHaas HW65F.
§Interpolated from data for dextran molecules of corresponding size from DePhillips and Lenhoff (2000).
‖Excluded volume calculated for $r = 1.55$ nm using $B_{HS} = 16/3\ \pi r^3$.

RESULTS

Lysozyme

To validate the model relating the retention factor and the second virial coefficient, we performed SIC experiments

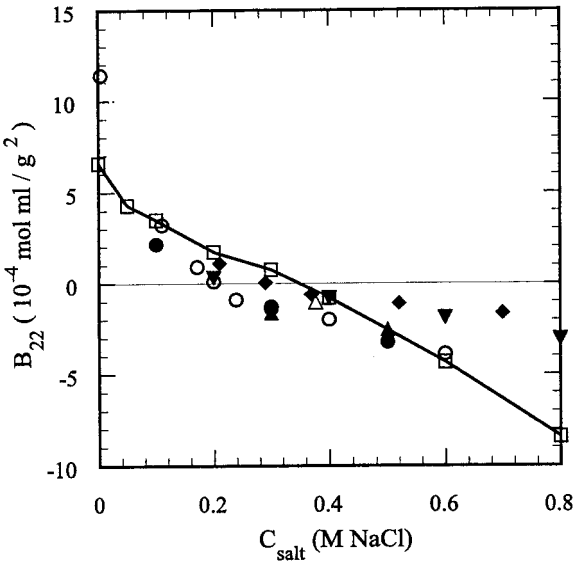

FIGURE 1 Lysozyme virial coefficients at pH 4.5 measured by SIC (□) and various scattering methods: ♦, Skouri (1993), ○, Rosenbaum and Zukoski (1996), △, Gripon et al. (1997), ●, Velev et al. (1998), ▲, Bonneté et al. (1999), and ▼, Piazza and Pierno (2000).

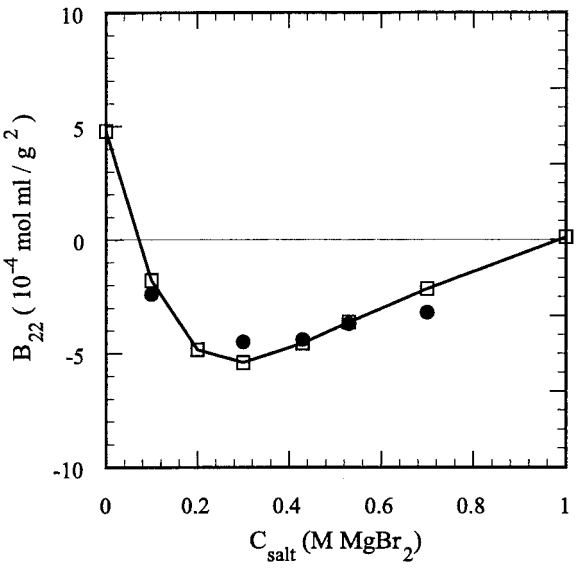

FIGURE 2 Lysozyme virial coefficients at pH 7.8 measured by SIC (□) and static light scattering (●, Guo et al., 1999).

over a wide range of pH (3–9) and ionic strengths (0.005–1 M). Fig. 1 compares our results with those from light and x-ray scattering at pH 4.5, corresponding to the conditions used most frequently in the literature. It should be noted that the light-scattering data are plotted as a function of concentration of sodium chloride, without considering the buffer concentration, and the pH at which the light-scattering data were collected range from 4.5 to 4.7. Without any adjustable parameters, the SIC and scattering data agree well, except at the extremes of low and high ionic strengths. At low ionic strengths ($<$0.05 M), the comparison of our results with scattering results is less meaningful because our experiments require a constant buffer concentration (5 mM), whereas for scattering experiments at low ionic strengths buffer is not required because the protein can buffer the solution, and therefore very low ionic strength conditions can be probed. Also, at low ionic strengths, long-range electrostatic repulsive interactions cause the measured retention volume to be smaller than the dead volume, and this exclusion effect is both difficult to measure accurately and weakly dependent on the amount of protein immobilized. At high ionic strength ($>$0.6 M), it is difficult to assess how significant is the deviation between the SIC and scattering results because there are appreciable variations in the scattering results reported by different investigators.

We also measured virial coefficients for lysozyme in magnesium bromide (Fig. 2), which shows a minimum in the virial coefficient values previously observed by SLS (Guo et al., 1999). The results agree closely with the SLS results and correctly predict the minimum in the virial coefficient at ~0.3 M $MgBr_2$. The reason that the B_{22} values become more positive at high ionic strength may be due to an increase in repulsive interactions due to binding of the divalent magnesium cation to the acidic residues of lysozyme, which has been suggested by others to explain lysozyme interactions in $MgCl_2$ solutions (Grigsby et al., 2000).

Table 2 contains a summary of the lysozyme virial coefficients measured by SIC and a comparison with light-scattering results. For 21 measurements, the average difference between SIC and scattering results was 1.7×10^{-4} mol ml/g^2, compared with an average internal difference among five different sets of scattering results of 0.9×10^{-4} mol ml/g^2 (Rosenbaum and Zukoski, 1996; Velev et al., 1998; Bonneté et al., 1999; Piazza and Pierno, 2000) at the same pH and sodium chloride concentrations. Although there are different thermodynamic variables held constant for the scattering (constant temperature, pressure, and number of particles) and SIC (flow system at constant temperature) measurements, the difference between thermodynamic conventions is expected to have only a small effect on virial coefficient values for proteins (Cabezas and O'Connell, 1993; Coen et al., 1995). Virial coefficients at pH 7 measured over 3 months after the column was initially packed changed ~0.3×10^{-4} mol ml/g^2, indicating that the particles were stable and gave reproducible results for months.

Chymotrypsinogen

We measured virial coefficients for chymotrypsinogen over a pH range from 3 to 6.8 and ionic strengths of 0.005–0.8 M. Chymotrypsinogen is known to be susceptible to cleav-

TABLE 2 Comparison of virial coefficients for lysozyme measured by SIC and SLS

pH	Electrolyte concentration (M)	B_{22} (10^{-4} mol ml/g^2) SIC	SLS	Reference
3	0.1	4.40	3.95	Velev et al., 1998
	0.3	2.49	0.55	Velev et al., 1998
	0.5	−0.36*	−1.26	Velev et al., 1998
4.5	0.1 M NaCl	3.31	3.23†	Rosenbaum et al., 1996
	0.2	1.44	0.15†	Rosenbaum et al., 1996
	0.3	0.40	−1.29†	Rosenbaum et al., 1996
	0.4	−1.25	−2.04†	Rosenbaum et al., 1996
	0.6	−5.02	−3.95†	Rosenbaum et al., 1996
6	0.1 M NaCl	2.12	−2.46	Velev et al., 1998
	0.3	−2.67	−3.60*	Velev et al., 1998
	0.5	−6.48*	−4.54	Velev et al., 1998
7	0.1 M NaCl	−0.41	−3.18*	Velev et al., 1998
	0.3	−6.44	−4.51*	Velev et al., 1998
	0.5	−9.39*	−5.61*	Velev et al., 1998
7.8	0.1 M $MgBr_2$	−2.30	−2.40	Guo et al., 1998
	0.3	−6.14	−4.50	Guo et al., 1998
	0.43	−5.24	−4.40	Guo et al., 1998
	0.53	−4.25	−3.70	Guo et al., 1998
	0.7	−2.70	−3.20	Guo et al., 1998
9	0.1 M NaCl	−3.21	−4.41	Velev et al., 1998
	0.3	−8.78	−5.28*	Velev et al., 1998
	0.5	−13.7*	−7.80	Velev et al., 1998

*Interpolated.
†pH 4.6.

age due to the autocatalytic activation of chymotrypsinogen to chymotrypsin above pH 5. However, we assayed the solutions for chymotrypsin enzymatic activity for 24 h at pH 7.5 by monitoring the rate at which chymotrypsin transforms α-benzoyl-L-tyrosine ethyl ester to α-benzoyl-L-tyrosine ethyl ester (Sun et al., 1996) and observed less than a 5% change. Therefore, because all our virial coefficient measurements were conducted below pH 7 and the samples were used within 24 h, we did not use any inhibitors to block the enzymatic activity of chymotrypsin. Inhibitors, such as phenylmethylsulfonyl fluoride (PMSF) (Gold and Fahrney, 1964), have been found to change the values of virial coefficients significantly (Velev et al., 1998).

Fig. 3 shows results at pH 3 for virial coefficient measurements of chymotrypsinogen compared with light-scattering (Velev et al., 1998) and osmometry (Pjura et al., 2000) results. The SIC results are in good agreement with literature results and show the correct trend. Fig. 4 shows corresponding results at pH 6.8, which shows an interesting change from repulsive to attractive interactions at low electrolyte concentrations previously seen in the literature (Velev et al., 1998). The origin of these strongly attractive electrostatic interactions has been modeled computationally and appears to be due to attractive electrostatic interactions present in a relatively small number of protein-protein configurations that show a high level of geometric complementarity and dominate the overall virial coefficient values (Neal et al., 1998).

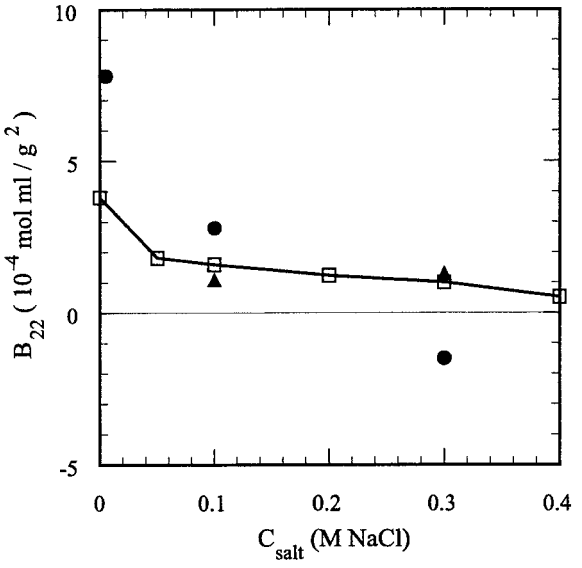

FIGURE 3 Chymotrypsinogen virial coefficients at pH 3 measured by SIC (□), static light scattering (●, Velev et al., 1998), and membrane osmometry (▲, Pjura et al., 2000).

Table 3 gives a summary of the chymotrypsinogen results and comparisons with literature data. For eight solution conditions, the average difference between virial coefficients measured by SIC and those from the literature (Velev et al., 1998; Pjura et al., 2000) is 1.2×10^{-4} mol ml/g^2, which compares favorably with an internal average difference of 2.5×10^{-4} mol ml/g^2 among the six sets of literature values at similar pH and sodium chloride concentrations. Similar results have been obtained by SIC for

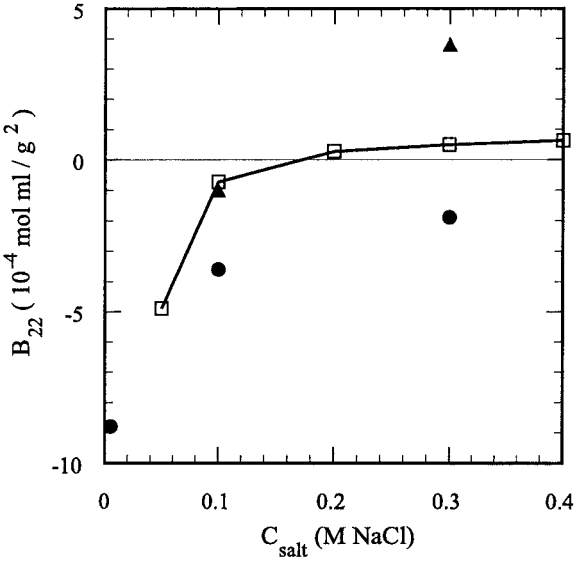

FIGURE 4 Chymotrypsinogen virial coefficients at pH 6.8 measured by SIC (□), static light scattering (●, Velev et al., 1998), and membrane osmometry (▲, Pjura et al., 2000).

TABLE 3 Comparison of virial coefficients measured by SIC, SLS, and membrane osmometry for chymotrypsinogen

pH	Electrolyte concentration (M NaCl)	B_{22} (10^{-4} mol ml/g^2) SIC	Literature values	Reference
3	0.1	1.59	2.80	Velev et al., 1998*
			1.10	Pjura et al., 2000†
	0.3	1.00	−1.50	Velev et al., 1998
			1.30	Pjura et al., 2000
4	0.1	1.04	−0.04	Velev et al., 1998
	0.3	0.40	−1.50	Velev et al., 1998
5	0.1	0.12	−1.40	Velev et al., 1998
			−2.00	Pjura et al., 2000
	0.3	0.16	−1.20	Velev et al., 1998
			−0.10	Pjura et al., 2000
6.8	0.1	−0.73	−4.10	Velev et al., 1998
			−1.00	Pjura et al., 2000
	0.3	0.49	−2.05	Velev et al., 1998
			3.80	Pjura et al., 2000

*SLS.
†Osmometry.

chymotrypsinogen immobilized on Sepharose particles (T. M. Przybycien, Carnegie-Mellon Univ., personal communication). The virial coefficients for chymotrypsinogen at pH 6.8 changed 0.1×10^{-4} mol ml/g^2 over 5 weeks, indicating that the column was stable and could be used for more than a month with little variability.

Chromatographic considerations

Lysozyme

The isocratic retention behavior of mobile lysozyme molecules interacting with immobilized molecules revealed a surprisingly strong dependence on both the surface coverage and the injection concentration. For most forms of chromatography (e.g., ion-exchange), the adsorption isotherm is linear at low injection concentrations and therefore the retention is independent of injection concentration. However, as the injection concentration is increased, the particle surface may become locally saturated and the retention volume varies with injection concentration (i.e., nonlinear chromatography). Fig. 5 shows that the opposite trend exists for lysozyme retention using SIC. At low injection concentrations, the retention was strongest, and as the injection concentration was increased, the peak maximum was shifted to the left, corresponding to lower retention, until it became independent of injection concentration (>12 mg/ml). The relative degree of peak tailing also changed from being very strong at low injection concentrations to being much weaker at higher injection concentrations. This behavior was more pronounced when the pH was closer to the isoelectric point of lysozyme (pH 11) and as the ionic strength was increased.

Fig. 6 shows a summary of the effects of injection concentration on the retention behavior for various levels of surface coverage. Particles without immobilized protein showed little effect of injection concentration on retention, confirming that the interactions among the mobile protein molecules even at 30 mg/ml were not responsible for the nonlinear retention behavior. The retention volume corresponding to the data in Fig. 6 for particles without any protein immobilized was 1.71 ± 0.01 ml over a concentration range of 1–30 mg/ml. For reference, the retention volume for chymotrypsinogen (26 kD), which is smaller than the size of a lysozyme dimer, was 1.64 ± 0.02 ml at 1

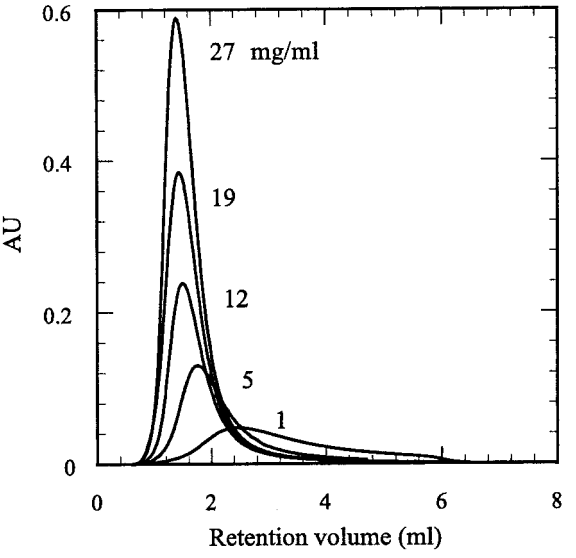

FIGURE 5 The effect of lysozyme injection concentration on peak shape and peak position at pH 7, 0.4 M NaCl, and 17 mg/ml lysozyme immobilized.

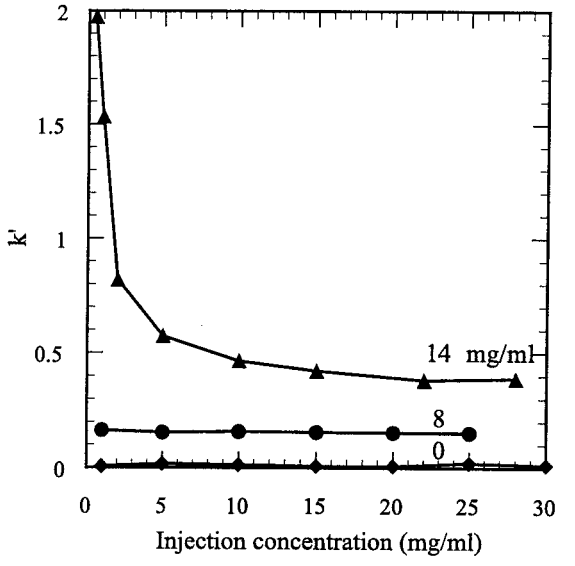

FIGURE 6 Summary of the effects of lysozyme injection concentration and surface coverage on the retention factor at pH 7 and 0.8 M NaCl.

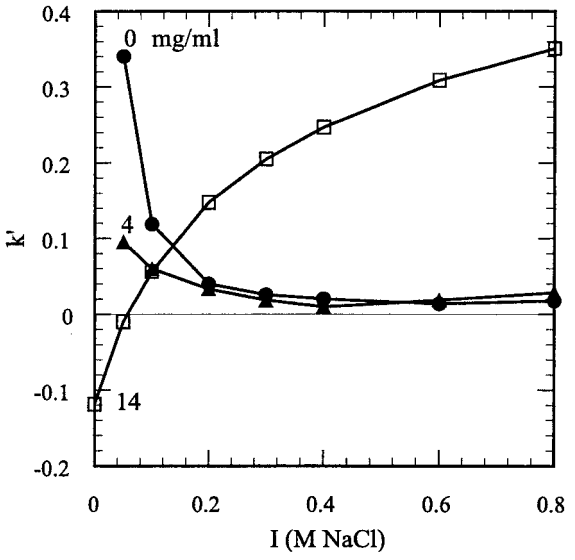

FIGURE 7 The effect of lysozyme surface coverage on the retention factor at pH 7.

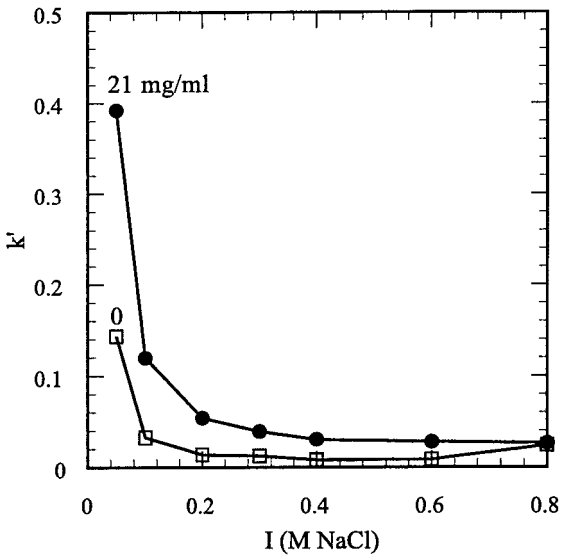

FIGURE 8 The effect of chymotrypsinogen surface coverage on the retention factor at pH 6.8.

mg/ml using the same column. The lack of deviation of the lysozyme measurements and the statistically significant difference relative to chymotrypsinogen suggests that any aggregation that might have occurred at high injection concentrations did not affect our measurements.

Even more interesting is the fact that at an immobilization density of 8 mg lysozyme/ml settled particles (18% surface coverage), the injection concentration also had little effect on the retention behavior. Yet when the immobilization density was raised to 14 mg/ml (33% surface coverage), there was a significant effect of injection concentration on retention behavior. The retention factor was reduced by a factor of five by increasing the injection concentration from 1 to 22 mg/ml, which impacted the measured virial coefficients significantly. The results shown in Figs. 1 and 2 and in Table 1 were performed at an injection concentration of 20 mg/ml and an immobilized concentration of 14 mg/ml, where there was little effect of injection concentration on retention.

Our choice of the surface coverage to use for measuring virial coefficients was based on the results in Fig. 7. For particles without immobilized protein or for particles with low surface coverage (9% surface coverage or 4 mg/ml), lysozyme was strongly retained at low ionic strengths due to nonspecific electrostatic interactions. However, at a higher surface coverage (14 mg/ml or 33% surface coverage), the retention was dramatically different. At low ionic strengths, the volume at which the protein was eluted was less than the dead volume of the column, indicating that repulsive interactions were present. Likewise, at high ionic strengths, the short-range attractive interactions dominated, resulting in the protein elution volume being significantly larger than the dead volume. A weaker, but still significant, dependence of surface coverage on retention was also observed at pH 4.5.

Chymotrypsinogen

The retention behavior of chymotrypsinogen was insensitive to both injection concentration and surface coverage, in stark contrast to lysozyme. Fig. 8 shows the effect of surface coverage on retention. The protein-surface interactions measured using particles without protein immobilized were very similar to the protein-protein interactions measured using particles with 21 mg/ml immobilized (43% surface coverage). However, because most of the available surface area of the particles was covered by chymotrypsinogen molecules, it is unlikely that the B_{22} measurements were strongly affected by nonspecific interactions. Finally, we did not explore different levels of surface coverage for chymotrypsinogen to obtain accurate virial coefficient measurements because our experience with lysozyme indicated that 30–40% surface coverage was optimal.

DISCUSSION

Model uncertainties

The relationship between the virial coefficient and the retention factor was derived for a single isolated, immobilized protein molecule interacting with a single mobile protein molecule, which was then scaled by the total number of immobilized protein molecules. At high immobilization concentrations, corresponding to near-monolayer surface coverage, immobilized protein molecules will have a smaller effective volume to interact with mobile protein

molecules than that assumed in this work (i.e., a hemisphere). For example, for adjacent molecules in contact, the volume of interaction (neglecting excluded volume effects) would be approximately one-third, not one-half, of the spherical volume. This would affect the final equation for B_{22} (Eq. 11) by increasing the prefactor in front of the retention factor from 1 to 1.5, which would cause the calculated B_{22} values to become more negative in the typical case of positive retention factors. In this work we have used particles with 30–40% of the surface covered (54.7% is the maximum surface coverage for spheres assuming random sequential adsorption (Feder, 1980)), which likely corresponds to a prefactor close to one. Due to the difficulties in interpreting retention results at high surface coverage, we suggest working at moderate surface coverage (i.e., 30–40%) where the assumption of a hemispherical volume of interaction is approximately valid. At much lower surface coverages nonspecific interactions with the base matrix can cause other kinds of discrepancies, as seen in Fig. 7.

Another uncertainty in the virial coefficient calculations is the excluded volume. It has been shown that the excluded volume of proteins calculated from the three-dimensional crystal structure is 1.7 times greater than the value calculated using the molecular volume and assuming a spherical shape, which is likely due to the surface roughness of the protein molecule (Neal and Lenhoff, 1995). The excluded volume calculated from the crystal structure relative to that calculated from the molecular volume provides an additional positive contribution to the virial coefficient, whereas the reduced volume of interaction per protein molecule caused by closely neighboring protein molecules generally provides a negative contribution. To make this method of general use we felt it was of significant importance to avoid the use of fitting parameters. Therefore, based on our experimental results and for simplicity, we used the molecular volume with the sphere approximation to calculate the excluded volume and the assumed the prefactor of one for the retention factor, which were likely offsetting contributions.

Finally, we have assumed that immobilized protein molecules are randomly oriented on the particle surface in view of the largely random distribution of primary amine groups (lysine and the N-terminus) on the surface. It is generally recognized that primary amines are more reactive when they are unprotonated (Haugland, 1996). Because the terminal amine has a lower pK_a (7–8) than the lysine residues ($pK_a \approx 10.5$), the reactivity of the terminal amine at neutral pH is generally thought to be higher. However, many factors can complicate selective immobilization of the terminal amine, such as accessibility. The relative reactivity of the terminal amine versus the side-chain amine groups has been studied for a 16-residue peptide with only one lysine residue in the middle of the peptide chain (Selo et al., 1996). At pH 6.5 the terminal amine was reacted only twice as frequently as the side-chain amine, even though the population of unprotonated terminal amines was 40 times that of the unprotonated side-chain amines. Even more interesting was that at pH 8.5, the lysine amine was favored over the terminal amine by approximately two to one, even though there were ~30 times more unprotonated terminal amine groups present than unprotonated side-chain amines. This study indicates that the relative fraction of unprotonated amines is not the sole indicator of amine reactivity.

In our experiments we performed our immobilization reaction at pH 7.5 for lysozyme and pH 8.5 for chymotrypsinogen. Although it is difficult to assess whether lysozyme molecules were more likely to be immobilized by the terminal amine at pH 7.5, carrying out the immobilization reaction at higher pH may further promote immobilization in random orientations, if this is compatible with protein and ligand stability (Haugland, 1996).

Effect of surface coverage

The fact that lysozyme retention was so strongly dependent on surface coverage at low ionic strengths (<0.1 M) was likely due to nonspecific interactions. However, the interesting retention behavior was at higher ionic strengths (>0.1 M), where there were attractive protein interactions. The surprising result was that beyond a threshold surface coverage (between 10 and 30% surface coverage), the retention behavior became strongly dependent on injection concentration. Model calculations of chromatographic retention with two interaction sites, in which the strongly adsorbing site is easily saturated and the weaker site is linear (i.e., amount adsorbed is proportional to amount in solution), predict peak tailing and significant shift in the peak maximum similar to that which we observed (Fornstedt et al., 1996). We hypothesize that as more protein is immobilized on the surface, the spacing between protein molecules decreases until immobilized proteins are so close that they can interact cooperatively with free protein molecules, giving rise to the strongly adsorbing sites proposed in the model. For the particles with 14 mg/ml lysozyme immobilized, there were apparently relatively few strongly adsorbing sites at which one free protein molecule could interact simultaneously with multiple immobilized proteins, because these nonlinear sites could be saturated easily by increasing the injection concentration. The second virial coefficient, which characterizes two-body interactions, could then be measured by studying the retention behavior of the linear, or two-body interaction, sites.

In a previous study (Ratnayake and Regnier, 1996), cation-exchange particles with higher levels of immobilized lysozyme than used here produced the opposite dependence of lysozyme retention versus surface coverage than we found. It is difficult to compare those results with ours due to differences in materials, characterization, and chromatography methods. However, it may be that at higher surface coverage lysozyme cannot interact with multiple proteins simultaneously at the surface, because there is not room for

a molecule to fit between immobilized protein molecules. It may be advantageous in the case of lysozyme to use a higher surface coverage than we did as this may allow lower injection concentrations to be used and therefore lower protein consumption.

The fact that chymotrypsinogen does not show the same strong retention dependence as lysozyme on injection concentration or surface coverage may be related to the lower propensity of chymotrypsinogen than lysozyme to crystallize. Lysozyme crystallizes in more than four space groups (Forsythe et al., 1999), suggesting a significant number of high-affinity pairwise configurations that can serve as crystal contacts. Chymotrypsinogen crystallizes in fewer space groups and much less readily (Pjura et al., 2000), indicating that there are likely fewer high-affinity contacts. It is the high-affinity configurations that contribute appreciably to B_{22} and to retention, and thus the larger number for lysozyme increases the probability of simultaneous binding to two immobilized molecules, even though the immobilized molecules are randomly oriented. The spacer arms on which the immobilized molecules are tethered allow some freedom of movement that may aid in such association.

The choice of the amount of injected protein (i.e., sample concentration and sample loop volume) should be guided by optimizing the peak symmetry. In the case of lysozyme, where retention depended strongly on injection concentration, our virial coefficient measurements were most accurate when we increased the injection concentration until the retention was independent of injection concentration and the amount of peak tailing was insignificant relative to the peak itself. The solubility of the protein provides an important experimental barrier to the highest injection concentration that can be used. We worked slightly above the solubility of lysozyme for a few virial coefficient measurements, which was possible because the time required for precipitation was typically several hours. Fig. 6 confirms that protein interactions between mobile protein molecules at high injection concentrations did not affect the retention behavior, because the retention is invariant with injection concentration using particles without immobilized protein under conditions at which lysozyme interactions are relatively strong. Both the 25 and 30 mg/ml samples were above the solubility limit for lysozyme at pH 7 and 0.8 M NaCl, yet gave results consistent with those below the solubility limit, which may have been due to the dilution of the sample after it was injected into the column.

Self-interaction chromatography versus static light scattering

The accuracy of our results compared with those from, for example, SLS should be evaluated in tandem with the time and the amount of protein required for the two methods. To obtain a single virial coefficient measurement by SLS, one would typically measure the scattered intensity versus protein concentration for five or more different protein concentrations ranging from 1 to 10 mg/ml (Velev et al., 1998). Typical glass ampoules that are used for light scattering require 1 ml of protein solution, adding up to a minimum of ~25 mg of protein per virial coefficient measurement. For our SIC experiments, a 1-ml column of particles required ~20 mg of immobilized protein. This could be reduced considerably by use of a miniaturized column. A single injection into the column gave one virial coefficient measurement, with each injection requiring 1 mg of lysozyme and 0.05 mg of chymotrypsinogen. Therefore, for a single virial coefficient measurement, SIC requires less protein than SLS, even including the amount of protein that must be immobilized. Furthermore, because the same column can be used for numerous virial coefficient measurements at different conditions, the consumption of protein for succeeding virial coefficients is an order magnitude less for lysozyme and more than two orders of magnitude less for chymotrypsinogen for SIC versus SLS. This is especially relevant for the common problem that the crystallization community faces when the structure of a newly discovered protein is desired, yet only milligrams of protein are available and solution conditions yielding protein crystals are unknown.

The time required to perform virial coefficient measurements is also important because the unrealistically long time required for screening hundreds of solution conditions is another reason that fundamental methods of predicting crystallization behavior have been underused. For example, traditional SLS requires ~1 day to obtain typically two or at the most three virial coefficient measurements without replication. SIC requires ~2 days to prepare the particles and pack the column, which then gives reproducible results for months. Each virial coefficient value can be obtained in ~45 min for columns of the size used in this work, even allowing for equilibration time between samples. Given the ease of automation in chromatography, this allows more than 30 virial coefficients to be collected per day on a single column with only a few hours of preparation time. This is an order of magnitude increase in efficiency for SIC compared with traditional light scattering.

Another significant additional advantage of SIC over SLS is that it is much less sensitive to experimental complications. Proteins scatter light weakly, and therefore scattering experiments are sensitive to dust or other impurities, so the success rate of measurements is lower for SLS than for SIC, where only the relative UV absorption is measured. Although others are currently working on flow systems using light scattering that allow similar data acquisition rates using a similar amount of protein relative to SIC (Asanov et al., 2000), we believe that miniaturized devices that utilize microfluidics will ultimately be most effective in terms of both time and protein. The principles of SIC appear to be more amenable to detecting protein interactions in lab-on-a-chip devices, because only the time the protein is retained

must be measured, which should be simpler to detect than the amount of light scattered.

Protein impurities and protein aggregates are also a common problem in light scattering. It is difficult to analyze scattering behavior from multi-component systems, as the scattering intensity is not a linear combination of the scattering from the individual components. This often confuses the interpretation of light-scattering results and can result in unrealistic molecular weights obtained by processing scattering results (Haynes et al., 1993; Curtis et al., 1998). This is also an important issue in light scattering from protein solutions with additives that are commonly used to crystallize proteins, such as polymers (e.g., polyethylene glycol) (Kulkarni et al., 2000) and surfactants (Hitscherich et al., 2000). Surfactants that are present at concentrations above the critical micellar concentration form micelles that contribute significantly to the scattered intensity; this is particularly important in crystallizing membrane proteins. Finally, many proteins are known to form dimers or higher-order structures (e.g., insulin) in solution, which also complicates the interpretation of scattering data. Yet in all these cases SIC provides the significant advantage of being insensitive to impurities, weakly binding additives, or higher-order aggregates because only the UV absorbance is measured instead of the scattered light. In fact, SIC could be used simultaneously to separate impurities or higher-order structures and to measure protein interactions, greatly simplifying the interpretation of the results relative to light scattering. However, complications can occur, such as strongly binding impurities to the molecule of interest, or overlapping peak maxima that cannot be individually resolved, although we have not experienced either of these problems in this work. Finally, only a low-pressure chromatography setup is required, which is more commonly available than other devices used to measure protein interactions.

The main disadvantage of SIC is that the same immobilized protein is used repeatedly for making virial coefficient measurements. Leakage of protein from the column or denaturation of the protein due to exposure to different solution conditions may occur. We did not observe either of these problems over several months, yet this is a concern with some immobilization chemistries, and therefore, further validation of this method is required. Finally, additives that irreversibly bind to proteins could accumulate on the immobilized molecules and therefore may interfere with accurate virial coefficient measurements.

CONCLUSIONS

We have demonstrated in this work that the osmotic second virial coefficient can be measured quantitatively by SIC. This method provides the significant advantages of being at least an order of magnitude less expensive in terms of the amount of protein and time required than conventional characterization methods, such as SLS. This is of particular importance due to the recent interest in measuring virial coefficients to find solution conditions that yield protein crystals. The crystallization community has underused the method of screening protein interactions to crystallize proteins due to the unrealistically high demands of protein and time presented by conventional methods. Our method moves this fundamental approach within the practical reach of crystallographers. We also believe that this type of retention-based characterization of protein interactions is more amenable to lab-on-a-chip devices than other more traditional approaches and therefore will become increasingly important as the push for miniaturized devices that utilize microfluidics continues in the coming years. Finally, SIC allows for the direct measurement of interactions between different protein molecules, which cannot be accomplished using any conventional characterization methods.

We are grateful for support from the National Science Foundation (grants BES-9510420 and BES-0078844), and from the National Aeronautics and Space Administration for a GSRP Fellowship to P.M.T.

REFERENCES

Asanov, A. N., D. B. Nikic, P. B. Oldham, and W. W. Wilson. 2000. A novel approach for investigating protein solution/crystal equilibrium. *In* 8th Int. Conf. Cryst. Biol. Macromol., Sandestin, FL.

Battistel, E., D. Bianchi, and G. Rialdi. 1991. Thermodynamics of immobilized ribonuclease-A. *Pure Appl. Chem.* 63:1483–1490.

Behlke, J., and O. Ristau. 1999. Analysis of the thermodynamic nonideality of proteins by sedimentation equilibrium experiments. *Biophys. Chem.* 76:13–23.

Bonneté, F., S. Finet, and A. Tardieu. 1999. Second virial coefficient: variations with lysozyme crystallization conditions. *J. Cryst. Growth.* 196:403–414.

Cabezas, H., and J. P. O'Connell. 1993. Some uses and misuses of thermodynamic models for dilute liquid solutions. *Ind. Eng. Chem. Res.* 32:2892–2904.

Cleland, J. L., M. F. Powell, and S. J. Shire. 1993. The development of stable protein formulations: a close look at protein aggregation, deamidation, and oxidation. *Crit. Rev. Ther. Drug.* 10:307–377.

Coen, C. J., H. W. Blanch, and J. M. Prausnitz. 1995. Salting-out of aqueous proteins: phase-equilibria and intermolecular potentials. *Am. Inst. Chem. Eng. J.* 41:996–1004.

Connolly, M. L. 1985. Molecular-surface triangulation. *J. Appl. Crystallogr.* 18:499–505.

Connolly, M. L. 1993. The molecular-surface package. *J. Mol. Graph.* 11:139–143.

Curtis, R. A., J. M. Prausnitz, and H. W. Blanch. 1998. Protein-protein and protein-salt interactions in aqueous protein solutions containing concentrated electrolytes. *Biotechnol. Bioeng.* 57:11–21.

DePhillips, P., and A. M. Lenhoff. 2000. Pore size distributions of cation-exchange adsorbents determined by inverse size-exclusion chromatography. *J. Chromatogr. A.* 883:39–54.

Ducruix, A., J. P. Guilloteau, M. Ries-Kautt, and A. Tardieu. 1996. Protein interactions as seen by solution x-ray scattering prior to crystallogenesis. *J. Cryst. Growth.* 168:28–39.

Durbin, S. D., and G. Feher. 1996. Protein crystallization. *Annu. Rev. Phys. Chem.* 47:171–204.

Fagerstam, L. G., A. Frostellkarlsson, R. Karlsson, B. Persson, and I. Ronnberg. 1992. Biospecific interaction analysis using surface-plasmon

resonance detection applied to kinetic, binding-site and concentration analysis. *J. Chromatogr.* 597:397–410.

Feder, J. 1980. Random sequential adsorption. *J. Theor. Biol.* 87:237–254.

Fornstedt, T., G. M. Zhong, and G. Guiochon. 1996. Peak tailing and slow mass transfer kinetics in nonlinear chromatography. *J. Chromatogr. A.* 742:55–68.

Forsythe, E. L., E. H. Snell, C. C. Malone, and M. L. Pusey. 1999. Crystallization of chicken egg white lysozyme from assorted sulfate salts. *J. Cryst. Growth.* 196:332–343.

Freyssinet, J. M., B. A. Lewis, J. J. Holbrook, and J. D. Shore. 1978. Protein-protein interactions in blood-clotting: use of polarization of fluorescence to measure dissociation of plasma factor-13a. *Biochem. J.* 169:403–410.

George, A., and W. W. Wilson. 1994. Predicting protein crystallization from a dilute-solution property. *Acta Crystallogr. D.* 50:361–365.

Gold, A. M., and D. Fahrney. 1964. Sulfonyl fluorides as inhibitors of esterases. II. Formation and reactions of phenylmethanesulfonyl a-chymotrypsin. *Biochemistry.* 3:783–791.

Grigsby, J. J., H. W. Blanch, and J. M. Prausnitz. 2000. Diffusivities of lysozyme in aqueous $MgCl_2$ solutions from dynamic light-scattering data: effect of protein and salt concentrations. *J. Phys. Chem. B.* 104: 3645–3650.

Gripon, C., L. Legrand, I. Rosenman, O. Vidal, M. C. Robert, and F. Boue. 1997. Lysozyme–lysozyme interactions in under- and supersaturated solutions: a simple relation between the second virial coefficients in H_2O and D_2O. *J. Cryst. Growth*. 178:575–584.

Guo, B., S. Kao, H. McDonald, A. Asanov, L. L. Combs, and W. W. Wilson. 1999. Correlation of second virial coefficients and solubilities useful in protein crystal growth. *J. Cryst. Growth.* 196:424–433.

Haugland, R. P. 1996. Handbook of Fluorescent Probes and Research Chemicals. Molecular Probes, Leiden, The Netherlands.

Haynes, C. A., F. J. Benitez, H. W. Blanch, and J. M. Prausnitz. 1993. Application of integral-equation theory to aqueous 2-phase partitioning systems. *Ann. Int. Chem. Eng. J.* 39:1539–1557.

Haynes, C. A., K. Tamura, H. R. Korfer, H. W. Blanch, and J. M. Prausnitz. 1992. Thermodynamic properties of aqueous alpha-chymotrypsin solutions from membrane osmometry measurements. *J. Phys. Chem.* 96:905–912.

Hill, T. L. 1960. An Introduction to Statistical Thermodynamics. Addison-Wesley, Reading, MA.

Hirsch, R. E., M. J. Lin, and R. L. Nagel. 1988. The inhibition of hemoglobin-C crystallization by hemoglobin-F. *J. Biol. Chem.* 263: 5936–5939.

Hitscherich, C., J. Kaplan, M. Allaman, J. Wiencek, and P. J. Loll. 2000. Static light scattering studies of OmpF porin: implications for integral membrane protein crystallization. *Protein Sci.* 9:1559–1566.

Kuehner, D. E., C. Heyer, C. Ramsch, U. M. Fornefeld, H. W. Blanch, and J. M. Prausnitz. 1997. Interactions of lysozyme in concentrated electrolyte solutions from dynamic light-scattering measurements. *Biophys. J.* 73:3211–3224.

Kulkarni, A. M., A. P. Chatterjee, K. S. Schweizer, and C. F. Zukoski. 2000. Effects of polyethylene glycol on protein interactions. *J. Chem. Phys.* 113:9863–9873.

McQuarrie, D. A. 1976. Statistical Mechanics. Harper Collins, New York.

Mukai, Y., E. Iritani, and T. Murase. 1998. Fractionation characteristics of binary protein mixtures by ultrafiltration. *Separation Sci. Technol.* 33: 169–185.

Neal, B. L., D. Asthagiri, and A. M. Lenhoff. 1998. Molecular origins of osmotic second virial coefficients of proteins. *Biophys. J.* 75: 2469–2477.

Neal, B. L., and A. M. Lenhoff. 1995. Excluded-volume contribution to the osmotic 2nd virial-coefficient for proteins. *Ann. Int. Chem. Eng. J.* 41:1010–1014.

Oakley, A. J., and M. C. J. Wilce. 2000. Macromolecular crystallography as a tool for investigating drug, enzyme and receptor interactions. *Clin. Exp. Pharmacol. P.* 27:145–151.

Patro, S. Y., and T. M. Przybycien. 1996. Self-interaction chromatography: a tool for the study of protein-protein interactions in bioprocessing environments. *Biotechnol. Bioeng.* 52:193–203.

Piazza, R., and M. Pierno. 2000. Protein interactions near crystallization: a microscopic approach to the hofmeister series. *J. Phys. Condens. Mater.* 12:A443–A449.

Pjura, P. E., A. M. Lenhoff, S. A. Leonard, and A. G. Gittis. 2000. Protein crystallization by design: chymotrypsinogen without precipitants. *J. Mol. Biol.* 300:235–239.

Plant, A. L., L. Locasciobrown, W. Haller, and R. A. Durst. 1991. Immobilization of binding-proteins on nonporous supports: comparison of protein loading, activity, and stability. *Appl. Biochem. Biotechnol.* 30: 83–98.

Porschel, H. V., and G. Damaschun. 1977. Determination of virial-coefficients of protein solutions by means of x-ray small-angle scattering and interpretations. *Stud. Biophys.* 62:69.

Ratnayake, C. K., and F. E. Regnier. 1996. Lateral interaction between electrostatically adsorbed and covalently immobilized proteins on the surface of cation-exchange sorbents. *J. Chromatogr. A.* 743:25–32.

Receveur, V., D. Durand, M. Desmadril, and P. Calmettes. 1998. Repulsive interparticle interactions in a denatured protein solution revealed by small angle neutron scattering. *FEBS Lett.* 426:57–61.

Rosenbaum, D. F., and C. F. Zukoski. 1996. Protein interactions and crystallization. *J. Cryst. Growth.* 169:752–758.

Schaink, H. M., and J. A. M. Smit. 2000. Determination of the osmotic second virial coefficient and the dimerization of beta-lactoglobulin in aqueous solutions with added salt at the isoelectric point. *Phys. Chem. Chem. Phys.* 2:1537–1541.

Selo, I., L. Negroni, C. Creminon, J. Grassi, and J. M. Wal. 1996. Preferential labeling of alpha-amino N-terminal groups in peptides by biotin, application to the detection of specific anti-peptide antibodies by enzyme immunoassays. *J. Immunol. Methods.* 199:127–138.

Skouri, M. 1993. "Autoassemblages d'electrolytes en solution aqueuses". Ph.D. thesis, Universite de Marrakech, Morocco.

Smith, M. H. 1970. Peptides and proteins. *In* Handbook of Biochemistry. H. A. Sober, editor. The Cleveland Rubber Co., Cleveland, OH. 71–98.

Sophianopoulos, A. J., C. K. Rhodes, D. N. Holcomb, and K. E. van Holde. 1962. Physical studies of lysozyme. I. Characterization. *J. Biol. Chem.* 237:1107–1112.

Ståhlberg, J., B. Jonsson, and C. Horvath. 1991. Theory for electrostatic interaction chromatography of proteins. *Anal. Chem.* 63:1867–1874.

Sun, Y., X. H. Jin, X. Y. Dong, K. Yu, and X. Z. Zhou. 1996. Immobilized chymotrypsin on reversibly precipitable polymerized liposome. *Appl. Biochem. Biotechnol.* 56:331–339.

Velev, O. D., E. W. Kaler, and A. M. Lenhoff. 1998. Protein interactions in solution characterized by light and neutron scattering: comparison of lysozyme and chymotrypsinogen. *Biophys. J.* 75:2682–2697.

Zhang, W. Z., and R. C. Augusteyn. 1994. On the interaction of alpha-crystallin with membranes. *Curr. Eye Res.* 13:225–230.

Zimm, B. H. 1946. Applications of the methods of molecular distribution to solutions of large molecules. *J. Chem. Phys.* 14:164–179.